RSC Advances

PAPER

View Article Online
View Journal | View Issue

Cite this: *RSC Adv.*, 2014, **4**, 16206

Enhancement of solar energy absorption using a plasmonic nanofluid based on TiO_2/Ag composite nanoparticles

Yimin Xuan,*[ab] Huiling Duan[b] and Qiang Li[b]

Received 22nd January 2014
Accepted 12th March 2014

DOI: 10.1039/c4ra00630e

www.rsc.org/advances

Combined with the solar irradiation spectrum, the optical properties of both TiO_2/Ag composite nanoparticles and water-based nanofluids composed of different nanoparticles are studied. The solar energy absorption features are compared among these nanofluids based on TiO_2, Ag and TiO_2/Ag composite nanoparticles. Due to the localized surface plasmon resonance (LSPR) effect excited on the Ag surface, the optical absorption of TiO_2/Ag plasmonic nanofluid is remarkably enhanced. The enhanced absorption by LSPR excitation is introduced in solar thermal conversion. The photothermal experiments of different nanofluids conducted under the same conditions reveal that TiO_2/Ag plasmonic nanofluid exhibits a higher temperature compared with that of TiO_2 based nanofluid. Although the temperatures of Ag nanofluid and TiO_2/Ag nanofluid are the same, the cost of TiO_2/Ag based nanofluid is much lower. The effect of nanoparticle concentration on the photothermal performance of TiO_2/Ag plasmonic nanofluid is also studied in this paper.

1. Introduction

Solar energy is the most abundant energy in the world. Due to the increasingly more serious energy problems, the effective utilization of solar energy becomes especially important. Solar energy can be converted to many other energy forms, such as electricity, chemical energy and thermal energy. Among the three different forms of energy conversion, solar thermal collectors that utilize solar radiation to generate thermal energy are the most straightforward and simplest energy conversion equipment. The conventional solar thermal collector is a surface-based flat plate receiver, which harvests solar energy with a highly absorbing surface.[1] Solar radiation is absorbed by this black surface and then transferred to the working fluid through convection and conduction. Therefore, the absorbing surface usually has a high temperature, which leads to significant radiative heat loss ($\propto T^4$), and consequently lowers the overall conversion efficiency, especially for applications involving concentrated solar collectors.

In order to decrease the heat loss at high temperature, Abdelrahman *et al.*[2] and Hunt[3] proposed a black-liquid collector in the 1970s. In contrast to the surface-based solar thermal collector, solar energy is directly absorbed by the working fluid in the black-liquid collector, so it is also called a volumetric solar thermal collector. Due to the absence of a highly absorbing surface in a volumetric solar receiver, the surface temperature is much lower than that of a surface-based solar thermal collector, so that the radiative heat loss can be reduced. Moreover, the overall thermal resistance is lowered since the thermal resistance from hot absorbing surface to working fluid is eliminated.[4,5]

For volumetric absorbers, the overall conversion efficiency is mainly limited by the optical absorption properties of the working fluid. Therefore, in order to improve the photothermal performance of solar utilization, first of all, it is necessary to enhance the light absorption characteristics of working fluids. Recently, nanofluid (nano-sized particles suspended in base fluid) has been introduced to solar thermal collectors as the working fluid that directly absorbs the solar radiation. Nanoparticles offer the potential of improving the absorption properties of liquids, leading to an increase in the photothermal efficiency. Taylor and co-workers[6] compared the extinction coefficients of different nanofluids by model predictions and spectroscopic measurements. They found that over 95% of incoming light can be absorbed with low nanoparticle volume fraction. Otanicar *et al.*[7] examined the photothermal efficiencies of nanofluids made from a variety of nanoparticles (carbon nanotubes, graphite, and silver). By controlling the size, shape, material, and volume fraction of the nanoparticles, the absorption spectrum can be tuned to maximize absorption of solar energy. An efficiency improvement of up to 5% was achieved using nanofluids as the absorption media. Saidur and co-workers[8] analyzed the effect of nanofluid on the efficiency of a direct solar collector, and investigated the absorption

[a]*School of Energy and Power Engineering, Nanjing University of Aeronautics and Astronautics, Nanjing 210016, China. E-mail: ymxuan@nuaa.edu.cn; Fax: +86 25 84890688; Tel: +86 25 84891512*

[b]*School of Energy and Power Engineering, Nanjing University of Science and Technology, Nanjing 210094, China*

properties of aluminum nanofluid by varying the particle size and volume fraction. With only 1% volume fraction, the aluminum nanofluid is almost opaque to light, and the efficiency improvement is promising.

Metal nanoparticles can excite localized surface plasmon resonance (LSPR) effects on their surfaces.[9–12] This resonant effect is excited when the oscillation frequency of electrons is consistent with the incident light frequency. At the resonance frequency, both the near electric-field properties and far-field absorption properties are strongly enhanced.[13–16] Therefore, combination of the LSPR effect of some noble metallic nanoparticles and the use of nanofluids leads to a new concept of plasmonic nanofluid. As the name implies, the plasmonic nanofluid is composed of plasmonic nanoparticles and base liquid. This new type of nanofluid can be used as working fluid in volumetric solar thermal collectors to enhance light absorption by means of the LSPR effect of the plasmonic nanoparticles suspended in the base fluid. Our previous work examined the absorption properties of plasmonic core/shell nanoparticle suspensions and theoretically revealed their potential application for solar energy harvesting.[17] Compared with nanoparticles of a single component, the plasmonic composite nanoparticles have many advantages, such as enhanced absorption of light and tuneable resonance frequency and intensity. Volumetric solar thermal receivers based on nanoparticles with a single component are widely studied. However, there are fewer studies on nanofluid solar thermal collectors based on plasmonic nanostructures. Lee *et al.*[1] theoretically studied the feasibility of a plasmonic nanofluid-based solar collector to enhance broad-band solar thermal absorption.

To improve the photothermal efficiency of nanofluid-based solar thermal collectors, the most important thing is to enhance the optical absorption of the nanofluid, which is affected by intrinsic optical properties of nanoparticles and their volume concentration.[1] In this paper, we prepare plasmonic hybrid nanoparticles and plasmonic nanofluids to experimentally explore the feasibility of making use of the LSPR effect to enhance solar thermal absorption. The optical properties of TiO_2/Ag composite nanoparticles and their suspension system are studied. Then, the photothermal performance of TiO_2/Ag nanofluid is examined under solar light irradiation and compared with other nanofluids.

2. Plasmon resonance effect

Under the illumination of incident light, the conductive electrons in a metal core are driven by the restoring force. If the oscillation frequency of electrons matches the frequency of the incident light, a plasmon resonance can arise.[9] The resonance modes excited on conductive nanoparticle surfaces are called LSPR. This can be excited by direct light illumination. The excitation of the LSPR effect is wavelength-dependent. In the electrostatic approximation, the complex polarizability α of a small nanoparticle of sub-wavelength diameter can be expressed as:[9]

$$\alpha = 4\pi R^3 \frac{\varepsilon - \varepsilon_m}{\varepsilon + 2\varepsilon_m} \quad (1)$$

where R is the particle radius, and ε and ε_m are the dielectric constants of the particle and environment respectively. It can be observed that the polarizability α can be resonantly enhanced if the denominator $|\varepsilon + 2\varepsilon_m|$ is a minimum. The condition that satisfies $\mathrm{Re}[\varepsilon(\omega)] + 2\varepsilon_m = 0$ is called the Fröhlich condition, under which the plasmon resonance can be excited.

When the LSPR effect is excited, an enhancement of light absorption and scattering at wavelengths corresponding to the plasmon resonance can be achieved. LSPR effect can localize energy in the vicinity of metals, leading to the electric field around a metal nanostructure being strongly enhanced. So that, based on the LSPR effect excited on metal surfaces, plasmonic nanostructures can be used to harvest solar energy for a variety of applications, such as solar cells, solar thermal collectors, photocatalytic applications and so on.

The resonance wavelength is dependent on particle shape, size and environment. By controlling the particle size, both the resonance wavelength and intensity can be tuned in a wide range of wavelengths.[10,18] Therefore, the spectrum can be selectively controlled by the utilization of the LSPR effect. By combining plasmonic nanostructures of different sizes and shapes, a broadband absorption spectrum may be obtained. Cole and Halas[19] determined the ideal distributions of spherical metallic nanoparticles to fit the solar spectrum at the earth's surface. Lv and coworkers[20] investigated the wavelength tuning ranges for different metallic shell nanoparticles and revealed that efficient spectral solar absorption fluids can be obtained using core/shell plasmonic nanoparticle suspensions. Based on the LSPR effect, it is possible to design plasmonic nanostructures for use in applications that require variable spectral absorption or scattering. In this paper, plasmonic nanoshells are used in photothermal considerations. Due to the LSPR effect excited on plasmonic nanoshells, a great enhancement of optical absorption is achieved.

3. Theoretical models

A schematic of the core/shell suspension system is shown in Fig. 1. The composite nanostructures made of TiO_2 core and Ag shell are dispersed randomly in water. It is known that photothermal performance is determined by the optical absorption of the nanofluid. So, the optical properties of both nanoparticles and nanofluid have to be examined.

3.1 Model of nanoparticles

In this study, the nanoparticles are assumed to be spherical, so their optical properties can be conveniently simulated based on Mie's theory. This method expands the internal and scattered fields into a set of normal modes described by vector harmonics. After a series of derivations, the scattering and extinction cross sections can be given by the following relations:[21]

$$C_{sca} = \frac{W_S}{I_i} = \frac{2\pi}{k^2} \sum_{n=1}^{\infty} (2n+1)\left(|a_n|^2 + |b_n|^2\right) \quad (2)$$

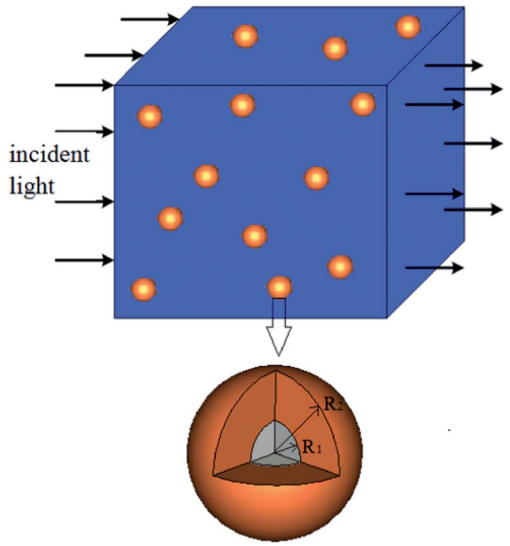

Fig. 1 Schematic of the core/shell suspension system, where nanoparticles are randomly dispersed in water.

$$C_{ext} = \frac{W_{ext}}{I_i} = \frac{2\pi}{k^2}\sum_{n=1}^{\infty}(2n+1)\mathrm{Re}(a_n + b_n) \quad (3)$$

Absorption cross section can be obtained using:

$$C_{abs} = C_{ext} - C_{sca} \quad (4)$$

where C_{sca}, C_{ext} and C_{abs} are scattering, extinction and absorption cross sections, k is wave number, and a_n and b_n are scattering coefficients for core/shell nanoparticle by considering the interference between forwardly and backwardly propagating spherical waves.[22]

The scattering and absorption cross sections are quantities concerning area, which are functions of particle size. Generally, scattering and absorption are evaluated by dimensionless efficiency factors Q_{sca} and Q_{abs} respectively. They are defined as the ratio of scattering or absorption cross section to geometrical cross section, as shown below:

$$Q_{sca} = \frac{C_{sca}}{\pi {R_2}^2} \quad (5)$$

$$Q_{abs} = \frac{C_{abs}}{\pi {R_2}^2} \quad (6)$$

The dielectric constants of Ag and TiO_2 materials are wavelength-dependent, which are obtained from ref. 23. The refractive index for water obtained from ref. 24 is also dependent upon wavelength in the near-infrared region.

3.2 Model of nanofluid

For the purpose of fully understanding the effects of suspended nanoparticles in a base fluid, the complete optical properties of the nanofluid are needed. Water is normally used as base fluid in solar thermal applications since it is non-toxic; however, its absorption is weak.[25] By suspending nanoparticles in it, the optical absorption can be improved. In this study, we suspend TiO_2/Ag nanoparticles in water composing the plasmonic nanofluid. The suspension system is shown in Fig. 1. Most of the available studies neglect the interactions between nanoparticles. They assume that the scattering from nanoparticles is independent. But, when concentration is high, interactions between nanoparticles may be significant. Especially for the plasmonic nanoparticle suspension system, both absorption and scattering are enhanced greatly as the LSPR effect is excited. Light scattered from one particle may be utilized by others, so that their interactions have to be taken into account.

In this work, the finite difference time domain method is used to simulate the optical properties of TiO_2/Ag nanofluid. This method is an explicit time marching algorithm used to solve Maxwell's curl equations on discretized spatial grids.[26] Based on this method, the propagation of electromagnetic waves within the suspension system can be simulated, so that inter-particle coupling inside the nanofluid is involved during computation. The electromagnetic propagation in nanofluid can be described by Maxwell's equations:

$$\varepsilon \frac{\partial \vec{E}}{\partial t} = \nabla \times \vec{H} - \vec{J} \quad (7)$$

$$\mu \frac{\partial \vec{H}}{\partial t} = -\nabla \times \vec{E} \quad (8)$$

$$\vec{J} = \sigma \vec{E} \quad (9)$$

where E and H are electric and magnetic fields, ε and μ are permittivity and permeability of medium, J is current density, and σ is conductivity.

These equations are solved on the discrete grids by replacing all the derivatives with finite-difference expressions. The discretization of the computational domain is usually based on the Yee grid.[27] Both the near-field and far-field properties can be conveniently calculated by this method. The reflection and transmission energies can be determined by the Poynting theorem:

$$\vec{S}_{ref} = \frac{1}{2}\mathrm{Re}\left[\vec{E}_{ref} \times \vec{H}^*_{ref}\right] \quad (10)$$

$$\vec{S}_{tr} = \frac{1}{2}\mathrm{Re}\left[\vec{E}_{tr} \times \vec{H}^*_{tr}\right] \quad (11)$$

where S_{ref} and S_{tr} are the time-averaged Poynting vectors corresponding to the reflected and transmission waves. Perfectly matched layers (PML) are imposed at the left and right surfaces along the light incident direction to absorb nearly all the incident waves. At other surfaces, periodic boundary conditions are imposed. The volume concentration of the nanoparticle suspension system is defined in the following form:

$$f = \frac{4N\pi R^3}{3V_{total}} \quad (12)$$

where N is the number of particles suspended in water.

4. Experimental section

4.1 Preparation of TiO_2/Ag plasmonic nanofluid

The plasmonic nanofluid was prepared by two steps. First, TiO_2/Ag composite nanoparticles had to be prepared. TiO_2 powders were provided by Deke Technology Company. According to ref. 28, TiO_2/Ag composite nanoparticles were synthesized by photochemical impregnation method. Ag nanoparticles were deposited on TiO_2 surface like islands. Then, TiO_2/Ag plasmonic nanofluid was prepared by adding a certain amount of the prepared composite nanoparticles to the base fluid. In order to ensure the TiO_2/Ag nanoparticles were uniformly dispersed in the base fluid, the dispersion system needed to be sonicated sufficiently.

4.2 Experimental setup

In this paper, the effect of concentration on photothermal performance of TiO_2/Ag plasmonic nanofluid is investigated experimentally. A schematic of the experimental setup is shown in Fig. 2. The size of the nanofluid container is 60 × 60 × 80 mm^3 with a square bottom surface. This container is made of glass and is coated with insulation materials except for the top surface. The top surface is covered with transparent glass. Sunlight is transmitted through the glass cover, then absorbed by TiO_2/Ag nanofluid. The temperature sensors chosen are measurement thermistor model 10K3MCD1 whose sizes are 3.3 mm long and 0.48 mm in diameter with a nominal resistance of 10 kΩ at 25 °C. They are located at different depths and different positions in the nanofluid. The average value is taken as the mean temperature of the nanofluid. The resistances of thermistors are measured using a Keithley model 2700 multimeter equipped with an 80-channel scanner by employing precise four-wire resistance measurements and low excitation current to minimize the thermistor self-heating. The resistance of thermistors is a function of temperature: by a simple mathematical conversion, the temperatures can be obtained. Solar irradiance intensity measured by a TES 1333R Solar Power Meter is recorded every minute.

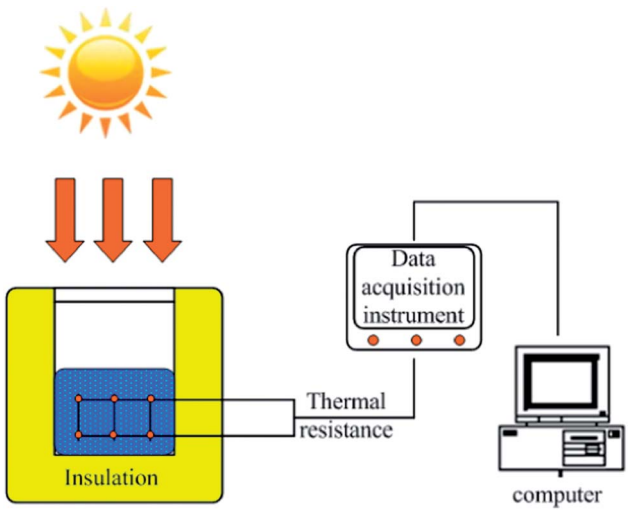

Fig. 2 Schematic of the experimental setup for solar thermal conversion.

The photothermal efficiency η can be estimated by:

$$\eta = \frac{mc_p(T_f - T_i)}{AG\Delta t} \quad (13)$$

where m is the mass of nanofluid, c_p is the specific heat of nanofluid measured by a Mettler Toledo DSC1 STAR^e system, T_i is initial temperature, T_f is final temperature, A is the top surface area of the receiver, G is the incident solar heat flux, and Δt is the time exposed to solar radiation.

5. Results and discussion

5.1 Optical properties of nanoparticles

In order to obtain an improvement of overall photothermal performance, the suspended nanoparticles have to be good absorbers of incident solar energy. TiO_2/Ag composite nanoparticle is studied in this work due to its unique optical properties. The simulated optical absorption of TiO_2 nanoparticle with $R = 30$ nm and that of TiO_2/Ag core/shell nanoparticle with $R_1/R_2 = 20/30$ nm are shown in Fig. 3(a).

Compared with solid TiO_2 nanoparticles, TiO_2/Ag composite nanoparticles exhibit enhanced optical absorption. It is caused by the LSPR effect excited on the Ag surface. LSPR is a resonant effect that originates from the collective oscillation of conductive electrons in metals. The collective oscillation frequency is called the resonance frequency. As shown in Fig. 3(a), two obvious resonance peaks can be observed at wavelengths of 360 nm and 630 nm. The electric field is greatly strengthened in the Ag shell at resonance wavelength (as shown in Fig. 3(b)), so that a remarkable enhancement of optical absorption can be obtained.[29]

The resonance frequency and intensity are dependent on the core and shell sizes. This sensitive dependence arises from the hybridization interaction between the plasmons of inner and outer metallic interfaces of the nanoshell.[19,30] Fig. 4 shows the spectral solar irradiance and absorption spectra of TiO_2/Ag nanoparticles with different core sizes. It can be observed that the solar irradiance is strongest in the visible light region. As core size increases, the resonance peak is red shifted, which gradually deviates from the strongest solar irradiation region. For the purpose of utilizing solar energy efficiently, the absorption spectra of nanoparticles should fit the solar spectrum at the earth's surface. As shown in Fig. 4, the absorption peak of TiO_2/Ag nanoparticles with $R_1/R_2 = 25/30$ nm is stronger than that of nanoparticles with other core sizes. However, its resonance wavelength is located at 840 nm where the solar irradiance is weaker. Although, the absorption peak of TiO_2/Ag nanoparticles with $R_1/R_2 = 20/30$ nm is weaker than that of nanoparticles with $R_1/R_2 = 25/30$ nm, the plasmon resonance of the former excited at 630 nm lies in the region where solar irradiance is strong. Therefore, for the core/shell nanoparticles with $R_1 = 20$ nm and $R_1 = 25$ nm, it is difficult to determine the preferred core size for which overall absorption of solar light is stronger from Fig. 4.

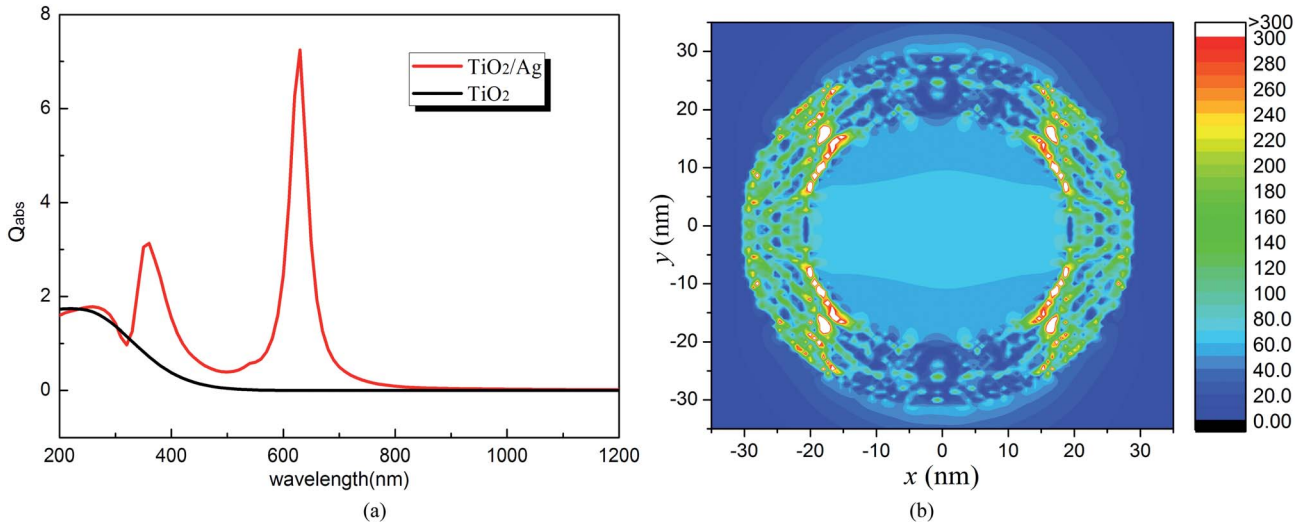

Fig. 3 (a) Absorption efficiency Q_{abs} of TiO_2/Ag core/shell nanoparticle and solid TiO_2 nanoparticle. (b) Electric field around TiO_2/Ag nanoparticle at $\lambda = 630$ nm. These results are obtained from the numerical simulation.

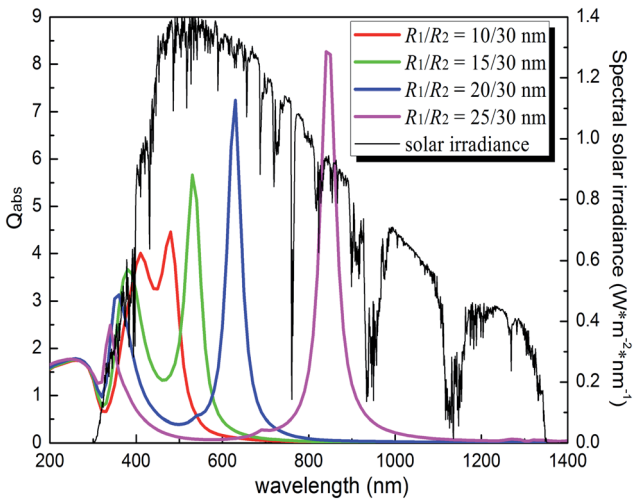

Fig. 4 Absorption efficiency Q_{abs} of TiO_2/Ag core/shell nanoparticles with different core sizes. Spectral solar irradiance is also presented.

The above analysis shows that TiO_2/Ag composite nanoparticle is an excellent optical absorber. Due to the LSPR effect excited on the Ag surface, the optical absorption is greatly enhanced. However, for nanofluid-based solar thermal application, the nanoparticles are randomly dispersed in base fluid, so that the optical properties of the nanofluid are also affected by nanoparticle concentration as well as interactions among nanoparticles. Therefore, besides the optical properties of single nanoparticles, the overall optical properties of the TiO_2/Ag plasmonic nanoparticle suspension system also need to be discussed. In Section 5.2, the absorbed solar energy is compared between nanofluids with nanoparticles of core sizes $R_1 = 20$ nm and $R_1 = 25$ nm. According to the overall absorbed energy, the preferred core size can be determined. The effect of concentration on overall absorption is discussed based on the nanoparticles with preferred core sizes.

5.2 Optical properties of nanofluid

To determine the effectiveness of nanofluids in solar applications, their absorption of solar energy must be established. The effect of nanoparticle material on overall absorptance is shown in Fig. 5. The optical absorption of nanofluids based on TiO_2, Ag and TiO_2/Ag composite nanoparticles is compared. They are studied under the condition of the same volume fraction $f = 0.01$. It can be observed that TiO_2 nanofluid mainly absorbs UV light in the region where solar irradiance is rather weak.

Compared with TiO_2 nanofluid, the absorption spectrum of Ag nanofluid is extended, which is mainly in the UV and visible light region. So, obviously, the absorption performance of Ag nanofluid is better than that of TiO_2 nanofluid. For nanofluid based on TiO_2/Ag composite nanoparticles, the absorption spectrum is further extended to longer wavelengths. As the core

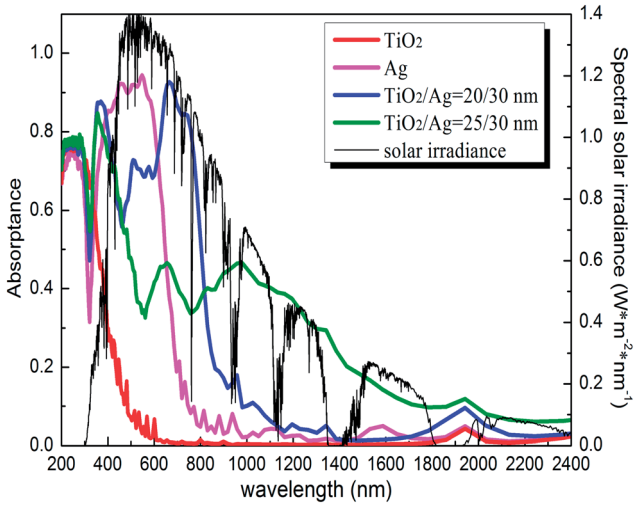

Fig. 5 Absorptance of nanofluids based on different nanoparticles (Ag, TiO_2 and TiO_2/Ag core/shell). The solar spectrum is also presented.

size increases from 20 nm to 25 nm, the absorption spectrum is broadened. This TiO_2/Ag plasmonic nanofluid can absorb light in a wide range of wavelengths (from UV to near-infrared). The curves in Fig. 5 imply that by selecting appropriate fractions of TiO_2/Ag hybrid nanoparticles with different sizes, one can enhance the absorption performance of plasmonic nanofluids within the near- and mid-infrared wavelength ranges.

To compare the absorption performance of different nanofluids, the solar energy absorbed should be determined. The energy absorbed by the nanofluid can be obtained from the following equation:

$$G_a = \int_{\lambda_1}^{\lambda_2} G_s(\lambda) \times A(\lambda) d\lambda \quad (14)$$

where G_a is the energy absorbed by the nanofluid, $G_s(\lambda)$ is the spectral solar irradiance, and $A(\lambda)$ is the absorptance of the nanofluid.

The integrated solar energies absorbed by different nanofluids are shown in Table 1. Among the four kinds of nanofluids, TiO_2/Ag nanofluid with R_1/R_2 = 20/30 nm absorbs the most energy. Accordingly, the overall absorption of nanofluid based on TiO_2/Ag composite nanoparticles is superior to that of nanofluid based on TiO_2 or Ag. Moreover, the energy absorbed by TiO_2/Ag nanofluid with nanoparticles of core size R_1 = 20 nm is larger than that with R_1 = 25 nm. Therefore, in the following discussion, the effects of volume fraction on overall absorption properties are explored based on TiO_2/Ag nanoparticles with R_1/R_2 = 20/30 nm.

The effect of volume fraction on optical absorptance of TiO_2/Ag nanofluid is shown in Fig. 6. It can be observed that TiO_2/Ag nanofluid mainly absorbs UV-visible light which accounts for about 47% of solar irradiation energy.[31] As volume fraction f increases, the absorptance of TiO_2/Ag based nanofluid gradually increases. When f varies from 0.005 to 0.01, the maximal absorptance increases from 0.757 to 0.928. The interactions among suspended nanoparticles are affected by nanoparticle concentration. More nanoparticles give rise to multi-scattering within the dispersion system and cause longer optical paths inside it. Then, enhanced light absorption can be obtained. On further increasing the volume fraction f to 0.015, the optical absorptance increases a little. Therefore, an optimal volume fraction may exist. For the optimal volume fraction, the optical absorption of nanofluid may be saturated. On further increasing the volume fraction, the absorption spectrum changes a little.

5.3 Photothermal performance of TiO_2/Ag nanofluid

The nanofluids based on Ag, TiO_2, and TiO_2/Ag composite nanoparticles are irradiated by solar light. They have the same volume fraction f = 0.005. Temperatures of these nanofluids are measured under the same condition. Fig. 7 shows the temperatures of different nanofluids varying with time.

Under solar light irradiation, the temperatures of nanofluids gradually increase with time. As solar radiation intensity weakens, the nanofluid temperatures also gradually decrease. Obviously, due to the optical absorption of nanoparticles, the temperatures of nanofluids are higher than that of deionized water. The maximal temperature of nanofluid based on TiO_2/Ag composite nanoparticles is the same as that of Ag nanofluid. It is much higher than the temperature of TiO_2 nanofluid, because the energy absorbed by TiO_2/Ag plasmonic nanofluid is much more than that absorbed by TiO_2 nanofluid (as shown in Fig. 5). Although the temperatures of TiO_2/Ag nanofluid and Ag nanofluid are the same, the cost of TiO_2/Ag nanofluid is lower than that of Ag nanofluid, since the amount of noble metal Ag

Table 1 Energy absorbed G_a by different nanofluids

Nanofluid	Energy absorbed G_a (W m^{-2})
TiO_2	57.89072
Ag	390.8815
TiO_2/Ag (20/30 nm)	484.9153
TiO_2/Ag (25/30 nm)	413.3601

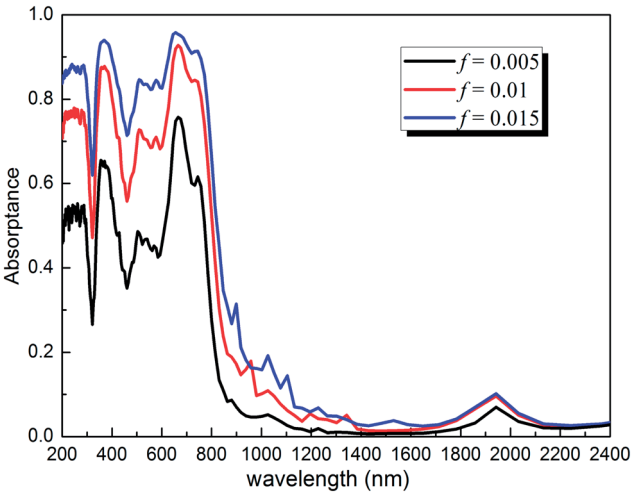

Fig. 6 Optical absorptance of TiO_2/Ag nanofluid as a function of volume fraction.

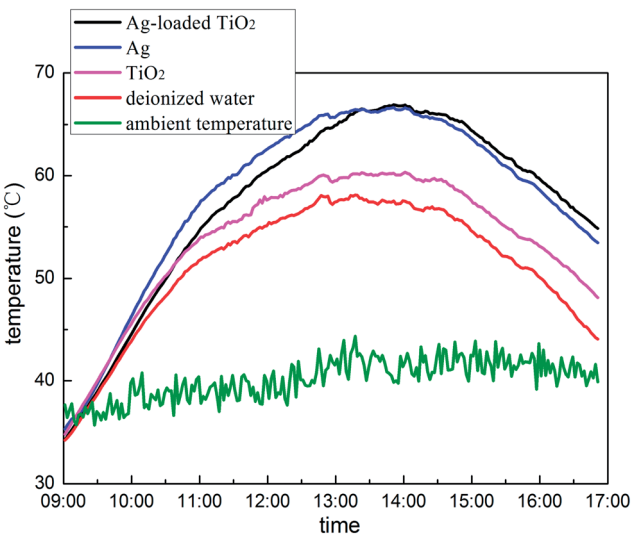

Fig. 7 Temperatures of different nanofluids as a function of time (f = 0.005).

Table 2 Photothermal efficiencies of nanofluids based on TiO_2, Ag and TiO_2/Ag nanoparticles as well as deionized water

Nanofluid	Average solar irradiation G (W m^{-2})	Specific heat c_p (J g^{-1} K^{-1})	Maximal temperature T_f (°C)	Photothermal efficiency η (%)
TiO_2	1004.122	3.89	60.21	16.07
Ag	1004.122	4.035	66.65	20.86
Ag-loaded TiO_2 ($f = 0.005$)	1004.122	4.01	66.93	20.9
Deionized water	1004.122	4.2	57.52	15.52

used in TiO_2/Ag nanofluid is less than that used in Ag nanofluid for the same volume fraction.

The photothermal conversion experiment based on different nanofluids is performed for the same solar irradiation and volume fraction. Photothermal efficiency can be estimated from eqn (13). Table 2 shows the thermophysical properties of various nanofluids, solar irradiation intensity as well as their corresponding photothermal efficiencies. Obviously, the photothermal efficiencies of nanofluids are higher than that of water without nanoparticles. The photothermal efficiency of nanofluid based on TiO_2/Ag nanoparticles is near to that of Ag nanofluid. It shows that their absorption performance is equivalent. However, TiO_2/Ag nanofluid has cost advantages.

5.4 Effect of concentration on photothermal performance

Due to the strong absorption of TiO_2/Ag composite nanoparticles, their corresponding nanofluid exhibits good photothermal performance. The effect of concentration on photothermal performance is studied based on TiO_2/Ag nanofluid. Under the same solar irradiation, the variation of temperature with time is measured for different volume fractions (as shown in Fig. 8). Among the four volume fractions examined, it can be observed that the temperature of nanofluid increases with volume fraction when $f < 0.01$, which is easy to understand. The amount of nanoparticles suspended in water increases with concentration, so that more light can be confined in the suspension system. The nanofluid with $f = 0.01$ exhibits the highest temperature. However, on further increasing the volume fraction to 0.015, the temperature decreases. As evident from the simulation results shown in Fig. 6, the optical absorption of the nanofluid somewhat increases when the volume fraction increases to 0.015. The absorption of light is almost saturated when the volume fraction further increases. Moreover, for nanofluid of high concentration, solar energy is mainly absorbed in a very shallow layer near the surface.[32] The inner layers are not directly heated by absorption of light, which is similar to the surface based solar thermal collector, leading to large heat loss from the hot surface.

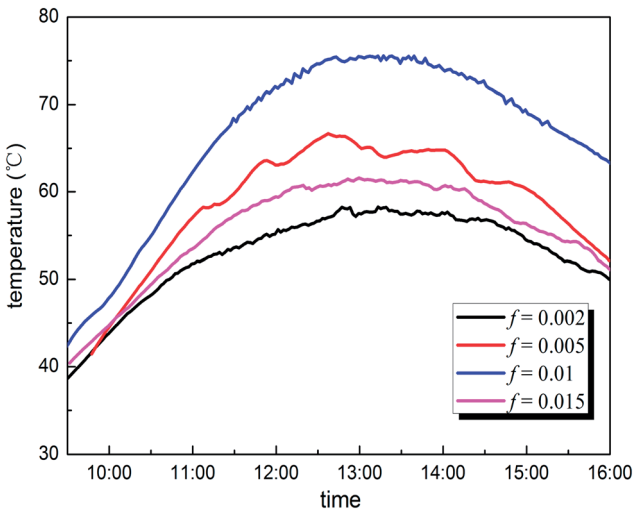

Fig. 8 Temperatures of TiO_2/Ag nanofluids with different concentrations as a function of time.

6. Conclusion

The feasibility of using plasmonic nanofluid has been experimentally explored. A TiO_2/Ag plasmonic nanofluid has been prepared by dispersing TiO_2/Ag composite nanoparticles in water. The optical properties of TiO_2/Ag nanoparticle and nanofluid have been studied, which indicates that TiO_2/Ag plasmonic nanoparticle is an admirable light absorber due to the LSPR effect excited on the Ag surface. In addition, photothermal conversion experiments have been performed for several different nanofluids. The temperature of TiO_2/Ag plasmonic nanofluid is much higher than that of TiO_2 nanofluid under the same incident light intensity. Although the temperature of TiO_2/Ag nanofluid is the same as that of Ag nanofluid, the nanofluid based on TiO_2/Ag composite nanoparticles has a cost advantage. TiO_2/Ag plasmonic nanofluid having good photothermal properties has potential applications in volumetric solar thermal receivers.

Acknowledgements

This work was financially supported by the National Natural Science Foundation of China (Grant no. 50936002) and the 333 scientific research project of Jiangsu Province (Grant no. BRA2011134). The authors thank Dr Ping Zhang for his help with experiments.

Notes and references

1 B. J. Lee, K. Park, T. Walsh and L. Xu, *J. Sol. Energy Eng.*, 2012, **134**, 021009.
2 M. Abdelrahman, P. Fumeaux and P. Suter, *Sol. Energy*, 1979, **22**, 45–48.

3 A. J. Hunt, *Small particle heat exchangers*, Lawrence Berkeley National Laboratory, 1978.
4 T. P. Otanicar, *Enhancing the heat transfer in energy systems from a volumetric approach*, Hawaii, 2011.
5 R. A. Taylor, P. E. Phelan, T. P. Otanicar, C. A. Walker, M. Nguyen, S. Trimble and R. Prashe, *Renewable Sustainable Energy Rev.*, 2011, **3**, 023104.
6 R. A. Taylor, P. E. Phelan, T. P. Otanicar, R. Adrian and R. Prasher, *Nanoscale Res. Lett.*, 2011, **6**, 225.
7 T. P. Otanicar, P. E. Phelan, R. S. Prasher, G. Rosengarten and R. A. Taylor, *J. Renewable Sustainable Energy*, 2010, **2**, 033102.
8 R. Saidur, T. C. Meng, Z. Said, M. Hasanuzzaman and A. Kamyar, *Int. J. Heat Mass Transfer*, 2012, **55**, 5899–5907.
9 S. A. Maier, *Plasmonics: Fundamentals and applications*, Springer, New York, 2006.
10 C. Noguez, *J. Phys. Chem. C*, 2007, **111**, 3806–3819.
11 J. Yao, A.-P. Le, S. K. Gray, J. S. Moore, J. A. Rogers and R. G. Nuzzo, *Adv. Mater.*, 2010, **22**, 1102–1110.
12 Y. Hu, R. C. Fleming and R. A. Drezek, *Opt. Express*, 2008, **16**, 19579–19591.
13 S. C. Warren and E. Thimsen, *Energy Environ. Sci.*, 2012, **5**, 5133–5146.
14 Y. Zhao and C. Burda, *Energy Environ. Sci.*, 2012, **5**, 5564–5576.
15 S. Chang, Q. Li, X. Xiao, K. Y. Wong and T. Chen, *Energy Environ. Sci.*, 2012, **5**, 9444–9448.
16 W. Hou, P. Pavaskar, Z. Liu, J. Theiss, M. Aykol and S. B. Cronin, *Energy Environ. Sci.*, 2011, **4**, 4650–4655.
17 H. Duan and Y. Xuan, *Appl. Energy*, 2014, **114**, 22–29.
18 K. L. Kelly, E. Coronado, L. L. Zhao and G. C. Schatz, *J. Phys. Chem. B*, 2003, **107**, 668–677.
19 J. R. Cole and N. J. Halas, *Appl. Phys. Lett.*, 2006, **89**, 153120.
20 W. Lv, P. E. Phelan, R. Swaminathan, T. P. Otanicar and R. A. Taylor, *J. Sol. Energy Eng.*, 2013, **135**, 021005.
21 C. F. Bohren and D. R. Huffman, *Absorption and Scattering of Light by Small Particles*, John Wiley & Sons, Inc, New York, 1998.
22 D. D. Smith and K. A. Fuller, *J. Opt. Soc. Am. B*, 2002, **19**, 2449–2455.
23 D. E. Palik, *Handbook of Optical Constants of Solids*, Academic Press Inc, London, 1985.
24 G. M. Hale and M. R. Querry, *Appl. Opt.*, 1973, **12**, 555–563.
25 T. P. Otanicar, P. E. Phelan and J. S. Golden, *Sol. Energy*, 2009, **83**, 969–977.
26 C. Oubre and P. Nordlander, *J. Phys. Chem. B*, 2004, **108**, 17740–17747.
27 K. S. Yee, *IEEE Trans. Antennas Propag.*, 1966, **14**, 302–307.
28 S. X. Liu, Z. P. Qu, X. W. Han and C. L. Sun, *Catal. Today*, 2004, **93**, 877–884.
29 V. E. Ferry, A. Polman and H. A. Atwater, *ACS Nano*, 2011, **5**, 10055–10064.
30 E. Prodan and P. Nordlander, *J. Chem. Phys.*, 2004, **120**, 5444–5454.
31 Q. Li, B. Guo, J. Yu, J. Ran, B. Zhang, H. Yan and J. R. Gong, *J. Am. Chem. Soc.*, 2011, **133**, 10878–10884.
32 E. Sani, S. Barison, C. Pagura, L. Mercatelli, P. Sansoni, D. Fontani, D. Jafrancesco and F. Francini, *Opt. Express*, 2010, **18**, 5179–5187.